ESEARCH ON AN IMPROVED PARTICLE SWARM OPTIMIZATION ALGORITHM FOR INVERSION OF ELEMENT YIELD IN PULSE NEUTRON GAMMA FORMATION ELEMENT LOGGING

by

Bo XIE [1,2,3,4]***, Lijiao ZHANG*** [3,4*]***, and Shangping XIE*** [5]

[1] School of Mechanical and Electronic Engineering, East China University of Technology, Nanchang, Jiangxi, China
[2] School of Information Engineering, East China University of Technology, Nanchang, Jiangxi, China
[3] Engineering Research Center of Nuclear Technology Application, East China University of Technology, Ministry of Education, Nanchang, China
[4] Laboratory on Radioactive Geoscience and Big Data Technology, East China University of Technology, Nanchang, Jiangxi, China
[5] School of Geophysics and Measurement-control Technology, East China University of Technology, Nanchang, Jiangxi, China

Scientific paper
https://doi.org/10.2298/NTRP2501037X

The physical problem of element yield inversion is transformed into a mathematical problem of solving overdetermined equations, then the particle swarm optimization algorithm is used to find the optimal solution of the system of equations to obtain the yield of formation elements. During the inversion process, relevant parameters such as the objective function, inertia weight factor, and learning factor are designed and optimized to make the particle swarm optimization algorithm more suitable for gamma spectrum signal processing, avoiding local extremum problems during the optimization process and improving the accuracy of element yield inversion. The calculation results show that compared with the traditional least squares method, the particle swarm optimization algorithm used in this paper can effectively invert the multi-peak gamma spectrum signal, with high inversion accuracy, and can effectively calculate the yield of trace elements.

Key words: neutron gamma logging, formation element, gamma spectrum, inversion of element yield, particle swarm optimization

INTRODUCTION

The gamma spectrum measured in neutron gamma formation element logging contains counts of various elements, and the gamma counts of each channel on the logging tool are linearly related to the gamma counts of each element in that channel.

If the number of measurement channels of the logging tool is n, then there are

$$\begin{bmatrix} N_1 \\ N_2 \\ \vdots \\ N_1 \end{bmatrix} = \begin{bmatrix} a_{11} & a_{12} & \dots & a_{1j} \\ a_{21} & a_{22} & \dots & a_{2j} \\ \vdots & \vdots & & \vdots \\ a_{i1} & a_{i2} & \dots & a_{ij} \end{bmatrix} \begin{bmatrix} y_1 \\ y_2 \\ \vdots \\ y_j \end{bmatrix} \quad (1)$$

where i is the measurement channel address, N_i – the total count of measurement channel i, y_j – the count of element j in that channel, and a_{ij} – the response coefficient of element j in channel i which is calculated using the element standard spectrum.

During the inversion process, there are errors in the measurement and calculation processes. Assuming that the error between the total count of each channel of the measuring instrument and the actual count of each element in that channel is ε_i (residual), eq. (1) becomes

$$\begin{bmatrix} N_1 \\ N_2 \\ \vdots \\ N_1 \end{bmatrix} = \begin{bmatrix} a_{11} & a_{12} & \dots & a_{1j} \\ a_{21} & a_{22} & \dots & a_{2j} \\ \vdots & \vdots & & \vdots \\ a_{i1} & a_{i2} & \dots & a_{ij} \end{bmatrix} \begin{bmatrix} y_1 \\ y_2 \\ \vdots \\ y_j \end{bmatrix} + \begin{bmatrix} \varepsilon_1 \\ \varepsilon_2 \\ \vdots \\ \varepsilon_i \end{bmatrix} \quad (2)$$

Equation (1) only has an accurate solution when the number of measurement channels of the logging tool is equal to the number of formation elements that need to be measured. However, in reality, the number of measurement channels in the instrument far exceeds the number of elements in the formation to be deter-

* Corresponding author, e-mail: lijiaozhang@ecut.edu.cn

mined. Therefore, eq. (1) is an overdetermined system of equations.

The least squares method is a commonly used approach for solving overdetermined systems of equations [1, 2]. The basic principle of the least squares method is to find a solution that minimizes the sum of squared errors and use it as the optimal solution for the overdetermined equation system. If the sum of squares of ε_i is SSR and the total number of channels in the measuring instrument is i, the calculation formula for SSR is

$$SSR = \sum_1^i \varepsilon_i^2 = \sum_1^i (N_i - \sum_1^i a_{ij,} y_j)^2 \quad (3)$$

The principle of the least squares method is simple and easy to implement, making it a widely used method for element yield inversion [3-8].

The gamma spectrum curve obtained from pulsed neutron gamma formation element logging is multimodal and solving it using the least squares method may lead to local extremum. In addition, in the actual inversion process, there may also be cases where the yield value is negative, which is inconsistent with the actual situation.

The processing of energy spectrum data encompasses a variety of methodologies [9-13], constituting a prominent research focus in the field of radiation measurement. In recent years, due to the continuous development of computing technology, various mathematical analysis methods and biologically intelligent evolutionary algorithms have gradually been applied to energy spectrum analysis. Among these algorithms, particle swarm optimization (PSO) searches for the optimal solution through cooperation and information-sharing among individuals in a population, demonstrating good parallelism and globality, rapid search speed, and a comprehensive search range. It is currently a trending research topic extensively applied in various fields [14-17].

The PSO is commonly used to find optimal solutions for non-linear, non-smooth, and multimodal functions, and is particularly suitable for extreme value calculations of gamma spectrum data with high randomness and multiple extrema [18,19]. This article aims to use the PSO algorithm to invert the element yield in pulse neutron gamma formation element logging.

PRINCIPLE OF PARTICLE SWARM OPTIMIZATION

In the PSO algorithm, the position of each particle is the solution of the objective function, and the quality of the solution is evaluated by fitness, which is determined by the objective function. All particles know their optimal position (local optimal solution, represented as pbest) and the current position they have experienced. Each particle knows the best position experienced by all particles so far (global optimal solution, represented as gbest). Each particle determines its next velocity (vector) [20, 21].

If the solution space is N-dimensional, the position of particle i is X^i, and the velocity is V^i

$$\begin{aligned} X^i &= (x_{i,1}\ x_{i,2} \cdots x_{i,N}) \\ V^i &= (x_{i,1}\ x_{i,2} \cdots x_{i,N}) \end{aligned} \quad (4)$$

Each particle updates its position and velocity based on the results of self-learning and group learning using eq. (5)

$$\begin{aligned} v_{i,j}(t+1) &= w v_{i,j}(t) + c_1 r_1 [p_{i,j}(t) - x_{i,j}(t)] + \\ &+ c_2 r_2 [p_{g,j}(t) - x_{i,j}(t)] \\ x_{i,j}(t+1) &= x_{i,j}(t) + v_{i,j}(t+1),\ \ j = 1,2,\ldots N \end{aligned} \quad (5)$$

where w is the inertia weight, c_1 – the self-learning factor, c_2 – the group learning factor, and the range of values for c_1 and c_2 is (0, 2), r_1 and r_2 are uniformly distributed random numbers within the interval of [0, 1]. Equation (5) is the core content of the PSO algorithm. All particles iterate according to this equation until the optimal solution is found.

According to eq. (5), to calculate the optimal solution of the objective function using PSO, key parameters such as determining the objective function, setting the initial position, weighting factors, and learning factors need to be determined. This article sets relevant parameters based on the characteristics of the energy spectrum signal obtained from pulse neutron gamma formation element logging.

Set objective function

This article constructs the objective optimization function based on the basic principle of the least squares method. Add constraints to ensure that the yield x and fitness of each element are not negative

$$\begin{aligned} \min f(x) &= \min \left(\sum_{i=1}^n (N_i - \sum_{j=1}^m a_{ij} x_j)^2\right) \\ x &\geq 0, s \geq 0 \end{aligned} \quad (6)$$

Set initial solution

In pulsed neutron gamma formation element logging, the gamma spectrum measured by the logging tool is a multimodal curve. Based on this characteristic, this article uses a set of Gaussian distribution signals as the initial solution. The distribution function of the Gaussian signal is

$$S(x) = a_1 e^{\frac{(x-b_1)^2}{2d_1^2}} + a_2 e^{\frac{(x-b_2)^2}{2d_2^2}} + a_3 e^{\frac{(x-b_3)^2}{2d_3^2}} + a_4 e^{\frac{(x-b_4)^2}{2d_4^2}} \quad (7)$$

where x is the channel address (x = 1, 2,..., 200); A Gaussian signal has four peaks (a_1, a_2, a_3, a_4), and the value of each peak is a random number within the interval [0, 1], b_1, b_2, b_3, b_4 are the channel addresses of the first peak, second peak, third peak, and fourth peak, d_1, d_2, d_3, d_4 are the standard deviation of each peak, taking random integer within the intervals [10, 20].

When $a_1 = 0.3$, $a_2 = 0.2$, $a_3 = 0.2$, $a_4 = 0.1$, $b_1 = 30$, $b_2 = 60$, $b_3 = 100$, $b_4 = 150$, $d_1 = 10$, $d_2 = 15$, $d_3 = 15$, $d_4 = 10$, the Gaussian signal is shown in fig. 1.

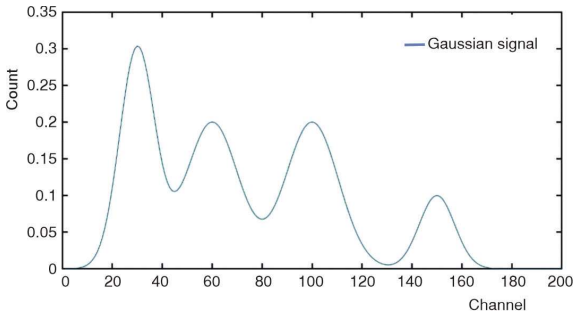

Figure 1. Initial solution signal

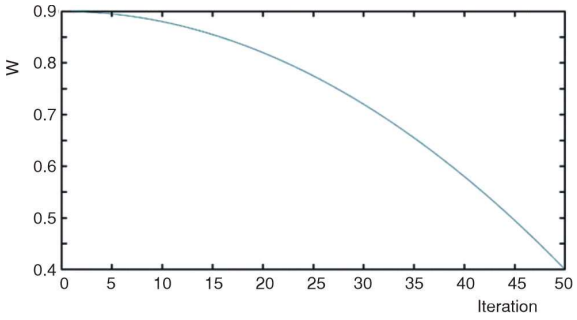

Figure 2. The trend of inertia weight factor changes

Inertia weight factor

As w increases, the search range of the algorithm expands, enhancing its global search ability, and speeding up convergence. However, the solution obtained may lack sufficient accuracy. When w is small, the algorithm's search range decreases, improving the effectiveness of local search and yielding a more accurate solution. However, this also increases the risk of getting trapped in local extrema. At the initial stage of inversion, due to the significant distance between random dissociation and the optimal solution, particles should move at a higher velocity to approach the optimal solution faster; After multiple iterations, the position of the particles may have approached the optimal solution. At this stage, the particles should move at a reduced speed to accurately search for the optimal solution within the local range. This article proposes a formula for calculating a variable inertia weight factor, designed to increase the particle's motion velocity during the initial stage of the process and decrease it in the later phase.

$$w = w_{\max} - (w_{\max} - w_{\min}) \cdot \left(\frac{t}{T}\right)^2 \tag{9}$$

where $w_{\max}$ (0.9) is the maximum weight, $w_{\min}$ (0.4) is the minimum weight, t (1, 2,..., 50) is the current number of iterations, and T (50) is the total number of iterations.

Learning factor

In the early stages of algorithm computation, particles primarily rely on self-learning due to their random initial positions, the notable separation between them, and their long distance from the optimal solution. During the later stage of algorithm computation, as the PSO search process continues, the global optimal solution is closer to the optimal solution, encouraging particles to group-learning [22-25]. The learning factor calculation formula used in this article is as follows

$$\begin{aligned} c_1 &= c_0 - (c_{\max} - c_0) \cdot \frac{t}{T} \\ c_2 &= c_0 + (c_{\max} - c_0) \cdot \frac{t}{T} \end{aligned} \tag{10}$$

where c_0 = 1.4962, which is the initial value of the learning factor, $c_{\max}$ = 2, which is the maximum value of the learning factor, t – the current number of times the algorithm has searched, and T – the total number of times the algorithm has searched. The value of the self-learning factor (c_1) gradually decreases from c_0 to 0.9924, the value of the group learning factor (c_2) gradually increases from c_0 to 2. Figure 3 shows the trend of changes in learning factors.

ELEMENT YIELD INVERSION

Rock standard spectrum simulation

In this article, experimental data is obtained through forward simulation. The composition ratio of rocks in the formation is shown in tab. 1.

Calculate response coefficient

To obtain the response coefficient (a_{ij}), it is necessary to simulate the standard spectra of the elements. Due to different elements having different inelastic scattering cross-sections and capture cross-sections, element yield inversion can be divided into inelastic spectra element yield inversion and capture spectra element yield inversion. The total number of channels in the energy spectra signal is 200. Calculate the yield of C, Al, Ca, Mg, O, and Si using gamma inelastic spectra; Calculate the yields of Al, Ca, Fe, K, Mg, Na, and Si using gamma capture spectra.

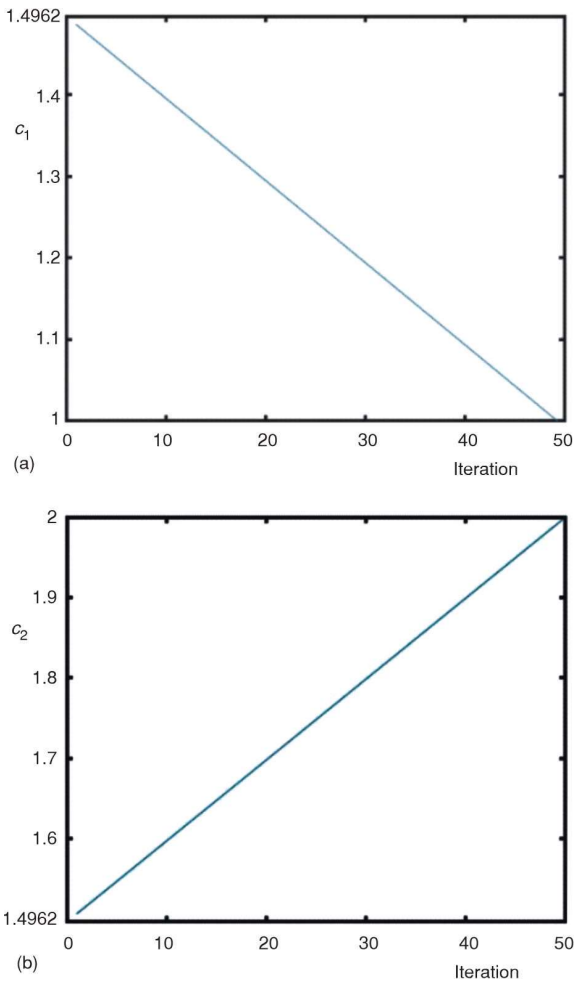

Figure 3. Trend of changes in learning factors; (a) self-learning factor and (b) group learning factor

Gamma inelastic standard spectra

When obtaining the standard spectra through numerical simulation, due to the inelastic scattering cross-sections of oxygen being $0.5 \cdot 10^{-28}$ m^2, water cannot be added to the well, and the formation material cannot be oxides. The geological material cannot be carbonate because the inelastic scattering cross-section of carbon element is $0.245 \cdot 10^{-28}$ m^2 [20, 21]. The setting of formation materials is shown in tab. 2.

After obtaining the gamma standard spectra through simulation, the inelastic spectra are separated using inelastic gates and then processed through denoising, background removal, and net spectra calculation. The final net spectra of the element standard spectra were obtained, as shown in fig. 4.

Gamma capture standard spectra

To obtain element capture spectra through simulation, it is necessary to ensure that the 14 MeV fast neutrons are completely slowed down before capture reactions occur between neutrons and the atomic nuclei that make up the formation material elements. Due to hydrogen being the strongest neutron moderator, pure water is used as the wellbore material. Due to the low absorption cross-sections of oxygen and carbon (with an absorption cross-section of 0.2 microbar for oxygen and 3.3 microbar for carbon), the contribution of oxygen and carbon to the capture spectrum is negligible, so the formation filling material is set as the oxide or carbonate of the target element. The setting of formation materials is shown in tab. 3.

Similar to inelastic spectra, after obtaining the formation spectrum through simulation, capture gates are used to separate the capture spectrum, followed by a series of processes such as denoising, background sub-

Table 2. Simulation conditions for inelastic standard spectra of elements

Element	Formation filling material	Inelastic cross-section [10^{-28} m^2]	Gamma characteristic energy [MeV]
C	$C_{22}H_{46}$	0.245	4.43
O	H_2O	0.5	6.13, 3.8
Si	Si	0.37	1.78
Ca	Ca	0.1	3.73
Al	Al	0.087	2.21
Mg	Mg	0.485	1.36

Table 1. Simulated lithological composition and proportion [%]

Mineral composition	Sand stone	Mudstone	Carbonate rocks	Gneiss	Granulite	Plagioclase amphibolite	Marble	Metamorphic mudstone
SiO_2	72.63	60.63	6.49	65.63	66.89	49.72	8.09	63.22
Al_2O_3	10.91	16.35	1.14	14.84	14.47	13.72	0.96	16.11
Fe_2O_3	2.46	4.33	0.35	2.03	2.23	4.38	0.26	3.06
FeO	1.09	1.42	0.32	2.73	2.12	7.6	0.33	2.75
Mg	1.26	1.86	6.53	2.15	1.94	7.35	10.56	2.08
CaO	2.52	2.66	42.84	3.26	2.7	9.11	39.14	1.59
Na_2O	1.41	0.8	0.1	3.64	3.19	2.48	0.11	1.3
K_2O	2.4	3.45	0.34	2.87	2.88	1	0.23	3.9
H_2O	2.56	4.56	0.74	1.34	1.88	2.1	1.02	3.26
CO_2	1.72	2.15	40.45	0.31	0.38	0.4	38.72	1.02

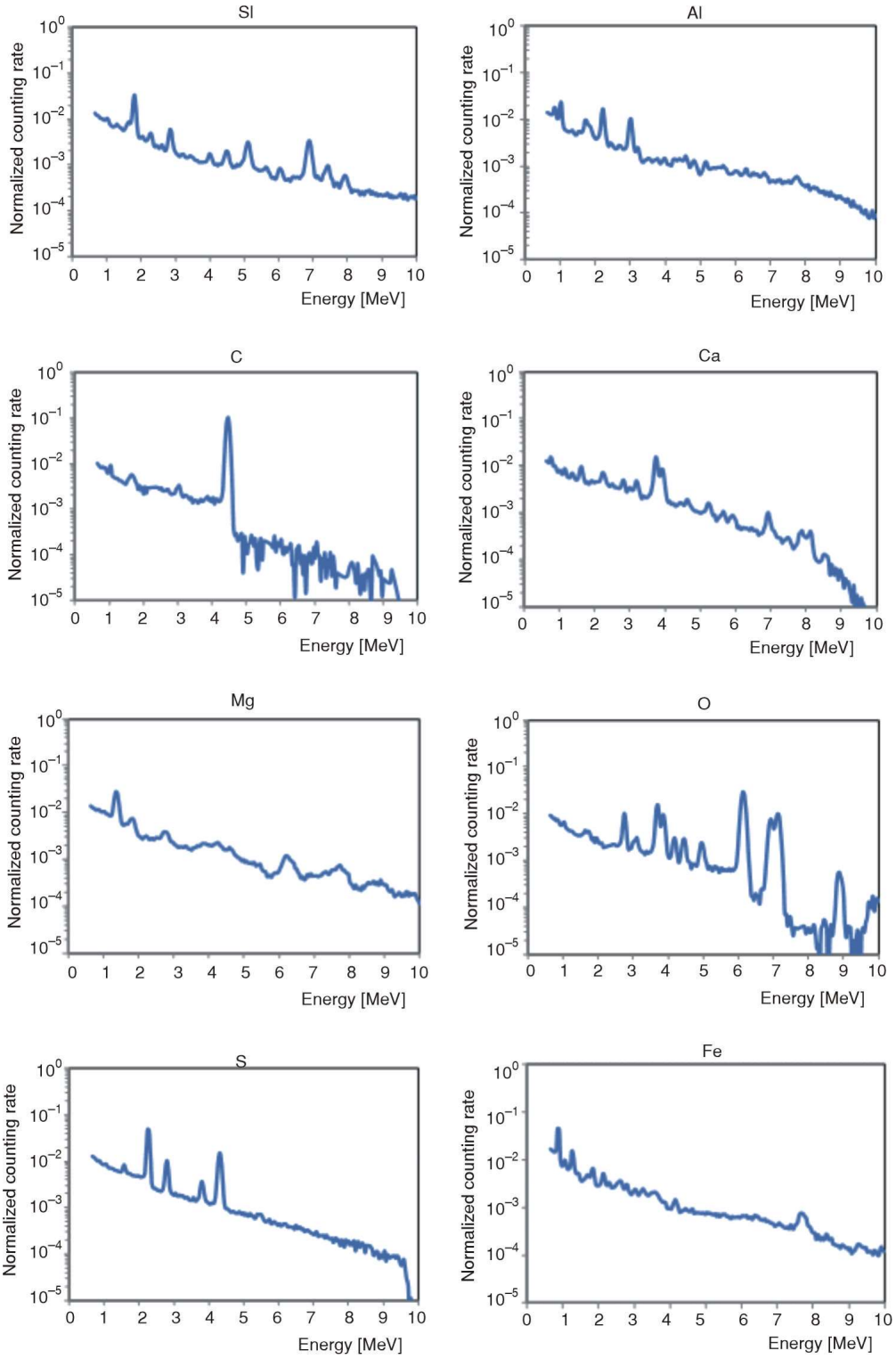

Figure 4. Standard inelastic net spectrum

traction, and net spectrum calculation to obtain the element standard capture spectrum, as shown in fig. 5.

Inversion of element yield for inelastic spectra

In the inversion of yield of inelastic elements, this paper uses simulated rock inelastic spectra as experimental data and calculates response coefficients using standard spectra. Use the least squares method and PSO algorithm for element yield inversion. In the inversion process of the PSO algorithm, the initial velocity and position matrices are both 6·100, and the Gaussian signal shown in fig. 1 is used as the initial solution. The initial value of velocity is a random value between intervals (0, 1). The least squares method and

Table 3. Simulation conditions for capture standard spectra

Element	Formation filling material	Inelastic cross-section [10^{-28} m^2]	Gamma characteristic energy [MeV]
H	H_2O	0.332	2.23
Si	SiO_2	0.16	3.54, 4.93, 6.38, 6.76, 7.19, 8.47
Ca	$CaCo_3$	0.43	1.94, 4.42, 6.42
Na	Na_2Co_3	0.534	3.587, 3.981, 6.395
Fe	Fe_2O_3	2.55	6.03,7.64
Al	Al_2O_3	0.230	3.02, 4.16, 4.79, 7.72
Mg	MgO	0.063	3.92
K	K_2Co_3	2.10	2.02, 5.73, 7.76

PSO algorithm were used to invert the element yield of the inelastic spectrum, and the inversion results are shown in tabs. 4 and 5.

Table 4 shows the results of element yield inversion using the least squares method for inelastic spectra. The elements with a higher proportion in the rock during simulation also have a higher yield in the inversion results. The yield of Si element obtained by inversion of granite, mudstone, gneiss, mudstone, sandstone, and plagioclase amphibolite is 24 % -27 %, and the yield of O element is 22 %-29 %. The yield of O in marble is 27 %, and the yield of Ca element is 18 %. The highest yielding elements in carbonate rocks are O (24 %) and Ca (24 %). The element yields of various rocks are consistent with the element ratios set during forward modeling. However, the yield of low-content elements (Mg, Fe, *etc*.) in the rocks obtained through inversion is inconsistent with the content ratio set by forward simulation. Indicating that the weighted least squares method is inaccurate in inverting the yield of elements with lower content.

Table 5 shows the results of using the PSO algorithm for yield inversion of inelastic spectral elements. The table indicates that the elements with higher yields in metamorphic rocks, metamorphic mudstone, gneiss, mudstone, sandstone, and plagioclase amphibolite are Si (22 %~28 %) and O (24 %~30 %). Elements with higher yields are O (28 %) and Ca (18 %). The inversion results of elements with high content in rocks closely resemble those obtained using the least squares method, indicating that the PSO algorithm used in this paper can effectively be used for the inversion of inelastic spectra.

Inversion of element yield for capture spectra

The process of capturing spectral element yield inversion is basically the same as that of inelastic spectral element yield inversion. However, in the inversion of element capture spectra, it is necessary to use capture standard spectra to calculate the response coefficients of elements. The least squares method and PSO algorithm were used to invert the element yield of the element capture spectra, and the inversion results are shown in tabs. 6 and .

In the results of least squares inversion, the highest yielding element in metamorphic rocks, metamorphic mudstone, gneiss, mudstone, sandstone, and amphibolite is Si (25 %~30 %). The element with the highest yield in marble and carbonate rocks is Ca (28 %, 30 %). The yields of iron elements in granulite, metamorphic mudstones, mudstones, gneiss, and plagioclase amphiboles are 9 %, 14 %, 9 %, 12 %, 24 %. The yield of K in metamorphic mudstone and gneiss is 16 %, and the yield of Al in plagioclase hornblende is 16 %. The yield of these elements is consistent with the element ratios set in the forward simulation. However, the yield of Mg in marble is relatively small, which does not match the magnesium content ratio set during the simulation.

In the inversion results of the PSO algorithm, Si is the most abundant element in metamorphic rocks, metamorphic mudstones, gneiss, mudstones, gneiss, sandstones, and plagioclase amphiboles, with a yield of 23 % to 30 %. The Ca is the most abundant element in marble and carbonate rocks, with a yield value of 28 % to 30 %. The yield of iron and aluminum elements is consistent with the element ratio set when simulating rock spectra, indicating that the PSO algorithm can be effectively used for element yield inversion of capture spectra. Compared with the least squares method, the PSO algorithm has a higher yield of Mg in rocks with higher content, indicating that the PSO method can effectively improve the recognition rate of Mg.

The results of inelastic and capture spectra inversion clearly demonstrate that the overall yield distribution of each element corresponds to the elemental content in the rock, indicating that the yield distribution is fundamentally reasonable. These findings confirm that the PSO algorithm discussed in this article can be effectively applied for element yield inversion of inelastic and capture spectra.

CONCLUSION

To make the PSO algorithm more suitable for inverting the energy spectrum data of pulse neutron gamma formation element logging, this paper proposes a new formula for calculating inertia weight, which reduces the inertia weight with increasing iteration times. Additionally, a new learning factor calculation function is introduced. As the search proceeds, the self-learning influence of particles gradually weakens, while the group-learning influence of particles gradually increases, effectively improving the convergence speed of the algorithm and the accuracy of the inversion results.

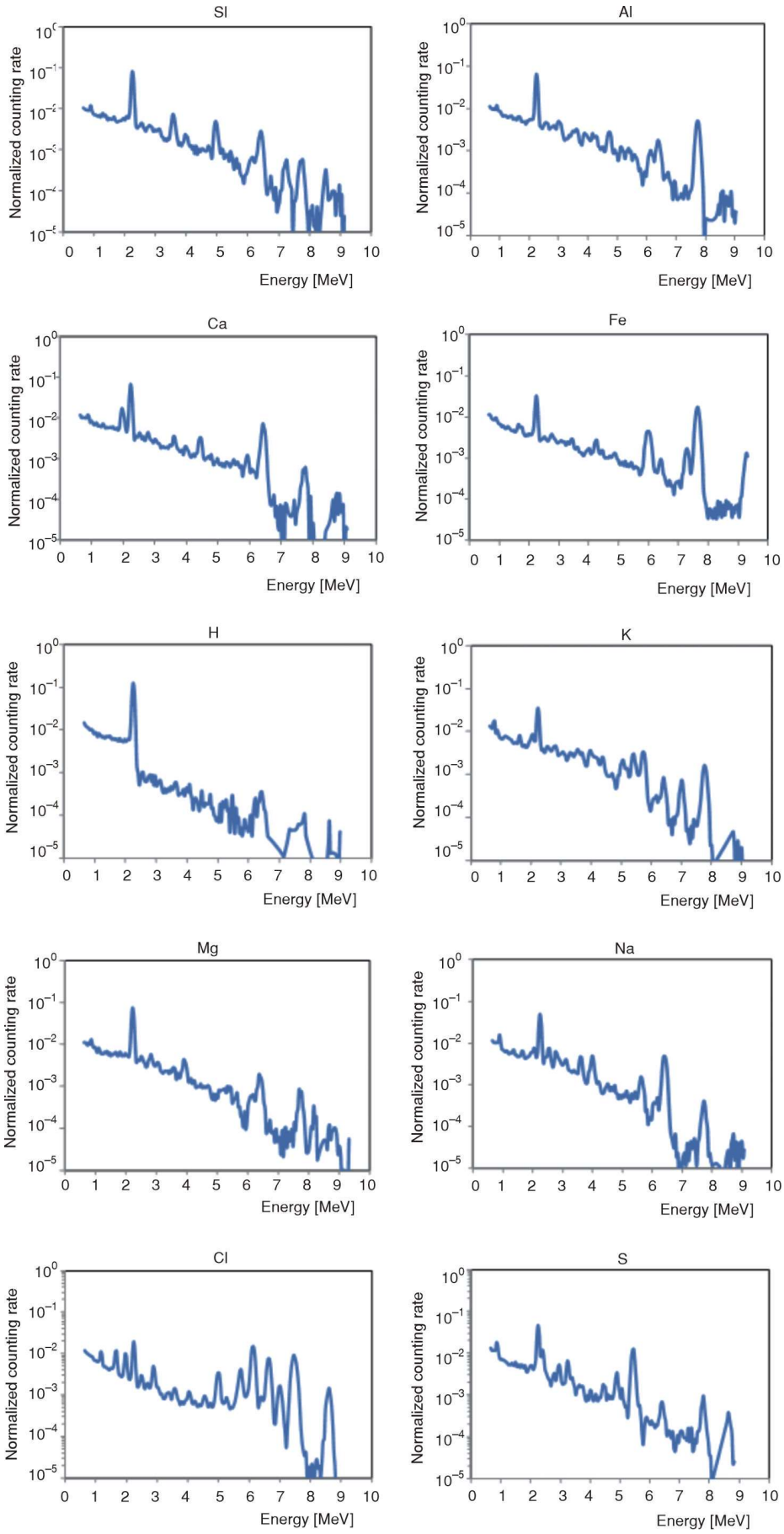

Figure 5. Standard capture net spectra

Table 4. Element yield of inelastic spectrum (least squares) [%]

Element	Granulite	Metamorphic mudstone	Marble	Mudstone	Gneiss	Sand stone	Carbonate rocks	Plagioclase amphibolite
C	0	0	0.03	0.01	0	0	0.04	0.02
Al	0.07	0.07	0	0.07	0.07	0.04	0	0.08
Ca	0.02	0.02	0.14	0.03	0.01	0	0.17	0.04
Mg	0.01	0	0.02	0.01	0.01	0.02	0.01	0.01
O	0.22	0.25	0.27	0.28	0.24	0.27	0.24	0.29
Si	0.24	0.25	0.03	0.27	0.26	0.25	0.02	0.26
Fe	0.01	0.01	0.01	0.01	0.02	0.02	0.01	0.08

Table 5. Element yield of inelastic spectrum (PSO) [%]

Element	Granulite	Metamorphic mudstone	Marble	Mudstone	Gneiss	Sand stone	Carbonate rocks	Plagioclase amphibolite
C	0.02	0.00	0.03	0.01	0.01	0.02	0.03	0.02
Al	0.05	0.06	0.01	0.07	0.08	0.05	0.03	0.08
Ca	0.02	0.02	0.18	0.04	0.02	0.02	0.19	0.04
Mg	0.01	0.01	0.02	0.02	0.02	0.02	0.02	0.02
O	0.24	0.29	0.28	0.29	0.27	0.30	0.28	0.25
Si	0.22	0.28	0.03	0.24	0.27	0.28	0.02	0.24
Fe	0.01	0.03	0.01	0.03	0.03	0.04	0.02	0.09

Table 6. Element yield of capture spectra (least squares) [%]

Element	Granulite	Metamorphic mudstone	Marble	Mudstone	Gneiss	Sand stone	Carbonate rocks	Plagioclase amphibolite
Al	0.06	0.08	0.02	0.09	0.11	0.08	0.01	0.16
Ca	0.01	0.02	0.28	0.04	0.02	0.04	0.35	0.05
Fe	0.09	0.14	0.01	0.09	0.12	0.02	0.01	0.24
K	0.04	0.16	0.02	0.11	0.21	0.07	0.01	0.03
Mg	0.03	0.01	0.06	0.02	0.04	0.05	0.02	0.03
Na	0.02	0.03	0.02	0.01	0.10	0.07	0.05	0.09
Si	0.28	0.25	0.04	0.28	0.29	0.34	0.06	0.24

Table 7. Element yield of capture spectra (PSO) [%]

Element	Granulite	Metamorphic mudstone	Marble	Mudstone	Gneiss	Sand stone	Carbonate rocks	Plagioclase amphibolite
Al	0.08	0.09	0.03	0.08	0.07	0.08	0.06	0.12
Ca	0.02	0.01	0.28	0.04	0.05	0.05	0.30	0.08
Fe	0.07	0.15	0.01	0.10	0.10	0.03	0.01	0.21
K	0.04	0.21	0.01	0.08	0.21	0.06	0.02	0.06
Mg	0.04	0.07	0.04	0.03	0.05	0.04	0.02	0.05
Na	0.04	0.05	0.02	0.02	0.13	0.07	0.01	0.08
Si	0.27	0.25	0.02	0.23	0.28	0.30	0.02	0.27

AUTHORS' CONTRIBUTIONS

B. Xie: guided the study design, performed data analysis, and drafted the initial manuscript. L. Zhang: developed methodologies and administered software/coding. S. Xie: supervised the project and secured funding.

ACKNOWLEDGEMENT

This work was supported by the Engineering Research Center of Nuclear Technology Application, Ministry of Education (No. HJSJYB2021-8), and Laboratory on Radioactive Geoscience and Big Data Technology (No. JELRGBDT201904).

ORCID NO

B. Xie: 0000-0002-8116-9814
L. Zhang: 0009-0004-7136-1142

REFERENCES

[1] Dongwei, H., *et al*., Application of High-Credible Statistical Results Calculation Scheme Based on Least Squares Quasi-Monte Carlo Method in Multimodal Stochastic Problems, *Computer Methods in Applied Mechanics and Engineering, Part B, 418* (2024), 116576
[2] Zhenghui, F., *et al*., Moving Window Sparse Partial Least Squares Method and its Application in Spectral

Data, *Chemometrics and Intelligent Laboratory Systems, 252* (2024), 105178
[3] Alireza, A. S., *et al*., Deep Learning in Standard Least-Squares Theory of Linear Models: Perspective, Development and Vision, *Engineering Applications of Artificial Intelligence, Part B, 138* (2024), 109376
[4] Qiang, Z., Exploneing for the Principle of Least Square Method and Its Treatment Method, *Metrology & Measurement Technique, 4*7 (2020), 4 pp. 75-76
[5] Hexi, W., *et al*., Analyzing Airborne Gamma-Ray Spectrum by the Least Square Method, *Nuclear Techniques, 39* (2016), 11, pp. 25-30
[6] Binghai, L., *et al*., Airborne Full-spectrum Data Processing and Application Effects, *Uranium Geology, 38* (2022), 6, pp. 1179-1186
[7] Qianming, H., *et al*., Progress in Research of Spectrum Unfolding Method on Neutron Spectrum Measurement, *Radiation Protection, 42* (2022), 4, pp. 265-279
[8] Xiaoliang, C., *et al*., Development and Validation of Neutron Spectrum Unfolding Code Based on Generalized Least Squares Method, *Atomic Energy Science and Technology, 49* (2015), 12, pp. 2195-2200
[9] Novković, D. N., *et al*., The Direct Measurement of ^{133}Ba Activity by the Sum-Peak Method, *Nuclear Instruments and Methods in Physics Research A, 608* (2009), 1, pp. 116-120
[10] Novković, D. N., *et al*., The Direct Activity Measurement of ^{133}Ba by Using HPGe Spectrometer, *Nucl Technol Radiat., 26* (2011), 1, pp. 64-68
[11] Gawad, K. A. E., *et al*., Optimization Approach of Gamma Spectrometer Measurements for Accurate Radioactive Materials Characterization, *Nucl Technol Radiat, 38* (2023), 3, pp. 187-193
[12] Yunlong, N., *et al*., Research on Energy Spectrum Anomaly Detection Method for State Control Radiation Environmental Monitoring Based on LOF algorithm, *Nucl Technol Radiat, 39* (2024), 1, pp. 47-57
[13] Yan, Z., *et al*., Andrea Codd, Inversion of 2-D Magnetotelluric (MT) Data with Axial Anisotropy using Adaptive Particle Swarm Optimization (PSO), *Journal of Applied Geophysics, 226* (2024), 105401
[14] Mewael, I., *et al*., Self-Adapting Control Parameters in Particle Swarm Optimization, *Applied Soft Computing, 8*3 (2019), 105653
[15] Alanna, M., *et al*., A Comparative Study of Evolutionary Algorithms and Particle Swarm Optimization Approaches for Constrained Multi-Objective Optimization Problems, *Swarm and Evolutionary Computation, 91* (2024), 101742
[16] Hüseyin, B., *et al.*, Dynamic Switched Crowding-Based Multi-Objective Particle Swarm Optimization Algorithm for Solving Multi-Objective AC-DC Optimal Power Flow Problem, *Applied Soft Computing, 166* (2024), 112155
[17] Wenbin, L., *et al*., Chaos Particle Swarm Optimization Algorithm for Optimization Problems, *International Journal of Pattern Recognition & Artificial Intelligence, 32* (2018), 11, 1859019-1-18
[18] Langdon, W. B., *et al*., Evolving Problems to Learn About Particle Swarm and Other Optimizers, *IEEE Transactions on Evolutionary Computation, 11* (2011), 5, pp. 561-578
[19] Alanna, M. N., *et al*., A Comparative Study of Evolutionary Algorithms and Particle Swarm Optimization Approaches for Constrained Multi-Objective Optimization Problems, *Swarm and Evolutionary Computation, 91* (2024), 101742
[20] Yu, T., *et al*., Multi-Subswarm Cooperative Particle Swarm Optimization Algorithm and its Application, *Information Sciences, 677* (2024), 120887
[21] Jose, D., *et al*., HYB-PARSIMONY: A Hybrid Approach Combining Particle Swarm Optimization and Genetic Algorithms to Find Parsimonious Models in High-Dimensional Datasets, *Neurocomputing, 560* (2023), 126840
[22] Sumit, B., *et al*., A Hybrid Particle Whale Optimization Algorithm with Application to Workflow Scheduling in Cloud-Fog Environment, *Decision Analytics Journal, 9* (2023), 100361
[23] Ibraheem, G. A. R., *et al*., A Novel Design of a Neural Network-Based Fractional PID Controller for Mobile Robots Using Hybridized Fruit Fly and Particle Swarm Optimization, *Complexity, 2020* (2020)
[24] Shusheng, W., *et al.*, Study of Monte Carlo Simulation on Optimally Designing Pulsing Neutron Formation Element Logging Tool, *Atomic Energy Science and Technology, 50* (2016), 8, pp. 1517-1523
[25] Yu, H., *et al*., Numerical Simulation and Method Study of X-Ray Litho-Density Logging, *Nuclear Science and Techniques, 31* (2020), 12, pp. 131-140

Received on November 7, 2024
Accepted on March 31, 2025

Бо СЈЕ, Лиђиао ЏАНГ, Шангпинг СЈЕ

ИСТРАЖИВАЊЕ ПОБОЉШАНОГ АЛГОРИТМА ОПТИМИЗАЦИЈЕ РОЈА ЧЕСТИЦА ЗА ИНВЕРЗИЈУ ПРИНОСА ЕЛЕМЕНАТА У ПУЛСНОМ НЕУТРОНСКОМ ГАМА ФОРМИРАЊУ ЕЛЕМЕНАТА

Физички проблем инверзије приноса елемената трансформише се у математички проблем решавања преодређених једначина. Затим се алгоритам оптимизације роја честица користи за проналажење оптималног решења система једначина, како би се добио принос формационих елемената. Током процеса инверзије, релевантни параметри као што су функција циља, тежински фактор инерције и фактор учења дизајнирани су и оптимизовани како би алгоритам оптимизације роја честица био погоднији за обраду сигнала гама спектра, избегавајући проблеме локалних екстрема током процеса оптимизације и побољшавајући тачност инверзије приноса елемената. Резултати прорачуна показују да, у поређењу са традиционалном методом најмањих квадрата, алгоритам оптимизације роја честица коришћен у овом раду може ефикасно инвертовати сигнал гама спектра са више пикова, са високом тачношћу инверзије и може ефикасно израчунати принос елемената у траговима.

Кључне речи: неутрон-гама логовање, елемент формације, гама спектар, инверзија приноса елемента, оптимизација роја честица